Proc. Natl. Acad. Sci. USA
Vol. 93, pp. 5688–5692, June 1996
Biochemistry

Minimizing a binding domain from protein A

ANDREW C. BRAISTED AND JAMES A. WELLS*

Department of Protein Engineering, Genentech, Inc., 460 Point San Bruno Boulevard, South San Francisco, CA 94080

Communicated by Peter G. Schultz, University of California, Berkeley, CA, February 1, 1996 (received for review November 22, 1995)

ABSTRACT **We present a systematic approach to minimizing the Z-domain of protein A, a three-helix bundle (59 residues total) that binds tightly (K_d = 10 nM) to the F_c portion of an immunoglobin IgG_1. Despite the fact that all the contacts seen in the x-ray structure of the complex with the IgG are derived from residues in the first two helices, when helix 3 is deleted, binding affinity is reduced $>10^5$-fold (K_d > 1 mM). By using structure-based design and phage display methods, we have iteratively improved the stability and binding affinity for a two-helix derivative, 33 residues in length, such that it binds IgG_1 with a K_d of 43 nM. This was accomplished by stepwise selection of random mutations from three regions of the truncated Z-peptide: the 4 hydrophobic residues from helix 1 and helix 2 that contacted helix 3 (the exoface), followed by 5 residues between helix 1 and helix 2 (the intraface), and lastly by 19 residues at or near the interface that interacts with F_c (the interface). As selected mutations from each region were compiled (12 in total), they led to progressive increases in affinity for IgG, and concomitant increases in α-helical content reflecting increased stabilization of the two-helix scaffold. Thus, by sequential increases in the stability of the structure and improvements in the quality of the intermolecular contacts, one can reduce larger binding domains to smaller ones. Such mini-protein binding domains are more amenable to synthetic chemistry and thus may be useful starting points for the design of smaller organic mimics. Smaller binding motifs also provide simplified and more tractable models for understanding determinants of protein function and stability.**

Protein domains are generally considered to be the smallest functional elements of protein structure, and often serve as portable modules that can create great diversity for protein–protein interactions (for reviews, see refs. 1 and 2). Here we show it is possible to make a functional protein domain substantially smaller, even when binding determinants are presented from distant sequences (a discontinuous epitope) that requires a stable protein fold. Through a systematic combination of structure-based design and phage display methods, we have engineered a stable two-helix binding domain from protein A that is about half the size, yet with nearly the same binding affinity, as the parent three-helix binding motif.

The B-domain of protein A, and a more stable variant called Z-domain (3), are three-helix, 59 residue modules that bind the F_c-portion of IgGs with a K_d of about 10–50 nM (4). X-ray (5), NMR (6), and mutational studies (4) show that binding contacts are presented from helix-1 (residues 7–18) and helix-2 (residues 20–38) (Fig. 1). Nonetheless, when helix 3 is deleted the remaining peptide loses its α-helical character, and binding affinity is reduced $>10^5$-fold (7). We reasoned that the two-helix motif might be stabilized and affinity optimized by improving three regions of the 38-residue peptide: the exposed hydrophobic region from helix 1 and helix 2 that contacted helix 3 (the exoface; see Fig. 2*A*), the buried residues between helix 1 and helix 2 (the intraface; see Fig. 2*B*), and the residues from the Z-domain predicted to contact the IgG (the interface; see Fig. 2*C*).

Given the uncertainties in predicting the consequences to stability and affinity for mutations in each of these regions, we felt that a random mutagenesis and selection method would be most appropriate. Phage display of protein or peptide libraries offers a powerful methodology for the selection of novel binding partners with improved affinity, altered specificity, or improved stability (for review, see ref. 8). High affinity proteins, displayed in a monovalent fashion as fusions with the M13 gene III coat protein (for review, see ref. 9), can be identified by cloning and sequencing the corresponding DNA packaged in the phagemid particles after a number of rounds of binding selection.

A functional Z-domain of protein A can be displayed on M13 phage particles (10, 11), and this binds with an EC_{50} of about 20 nM to IgG. Starting with a peptide representing the first two helices of the Z-domain, we constructed phagemid libraries at the exoface, intraface, and interface. The libraries were selected sequentially and combined such that the best selectant from the exoface library was used as a starting scaffold for the intraface library, and the best selectant from that was incorporated into the starting scaffold for the interface library. Through successive compilation of selected mutations, we evolved a peptide that binds IgG_1 with nearly the same affinity as the wild-type Z-domain yet is about half the size.

MATERIALS AND METHODS

Construction of Libraries. Monovalent phagemid libraries (12) of the truncated Z peptide were generated by site-directed mutagenesis (13). Each library contained four or five codons fully randomized for all 20 amino acids (see Table 1). The starting template for libraries 2 and 3 included a frame shift as well as a TAA stop codon to eliminate the background wild-type clones. Stocks of $\approx 10^{14}$ phagemids per ml were prepared from PEG precipitates of culture broths from XL-1 Blue cells containing the plasmid and superinfected with KO7 helper phage.

Selection and Analysis of IgG-Specific Phagemids. Microtiter plates (Maxisorb, 96-well; Nunc) were coated with human IgG (Zymed) at a concentration of 10 μg per ml in 50 mM sodium carbonate pH 9.6 overnight at 4°C. Wells were blocked with a 1:1 mixture of 50 mM sodium carbonate (pH 9.6) and binding buffer (phosphate-buffered saline (PBS) (pH 7.2), with 0.1% bovine serum albumin (Sigma, globulin free) and 0.05% Tween 20 (Sigma) for 1 h. Approximately 10^{12} phage from the appropriate stock diluted to 100 μl with binding buffer were incubated for 2 h before washing 20 times with PBS containing 0.05% Tween 20. Bound phage were eluted with 100 μl of 0.2 M glycine (pH 2.0), neutralized with 1 M Tris (pH 9.0), and then used to infect *Escherichia coli* (XL-1 Blue; Stratagene) for phagemid production. Phage ELISA were determined as described (14) against human IgG coated at 10 μg per ml in microtiter plates using an anti-M13-horseradish peroxidase conjugate (Pharmacia) with an *o*-phenylene diamine substrate (Sigma). Clones of interest were transformed

The publication costs of this article were defrayed in part by page charge payment. This article must therefore be hereby marked "*advertisement*" in accordance with 18 U.S.C. §1734 solely to indicate this fact.

*To whom reprint requests should be addressed.

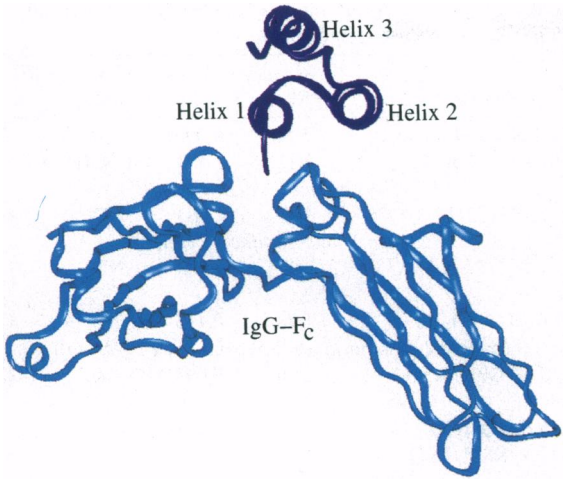

FIG. 1. Ribbon diagram of the B-domain of protein A (blue) in complex with the CH2, CH3 fragment of an IgG_1 (gray) taken from x-ray coordinates (5). Helix 3 appears disordered in the crystal structure, although NMR experiments indicate that it is in fact helical (6). In this figure, helix 3 has been modeled as a helix.

into 27C7 cells (a nonsuppressor strain of *E. coli*), and 250 ml cultures were grown in low phosphate AP5 minimal medium for 16 h (15). Both the supernatants and the periplasmic shockates were purified by affinity chromatography on IgG-Sepharose (Pharmacia). Final purification was accomplished by reverse-phase HPLC. The mass of each peptide was confirmed by electrospray mass spectrometry, and peptides were >95% pure by HPLC. Peptide concentrations were determined by quantitative amino acid analysis.

Binding Kinetics and Circular Dichroism (CD) Studies. Association and dissociation rate constants for the binding of both Z-domain and the selected peptides were determined by surface plasmon resonance. A monoclonal IgG_1 (anti-HER-2; Genentech) was immobilized on the biosensor chip covalently through the primary amines (16). A coupling density of ≈6000 RUs was used for both association and dissociation constant determinations. Association and dissociation rates (see Table 2) were measured at a flow rates of 20 and 25 μl/min, respectively, in PBS buffer (pH 7.4) with 0.05% Tween 20 (17).

CD spectra were recorded on an Aviv Associates (Lakewood, NJ) model 60DS spectropolarimeter in the wavelength range of 250–190 nm in 0.2-nm intervals in a thermostated circular cuvette with a path length of 0.05 cm. The final CD spectra represent an average of three scans with an integration time of 2 s. Results are reported as mean residue ellipticity $[\theta]_{MRW}$, in deg·cm^2·dmol^{-1}). Spectra were recorded at 8°C with peptide concentrations of 0.20 mg/ml in 100 mM sodium chloride and 10 mM Tris·HCl (pH 7.2). Curve fitting was accomplished by using the method of Provencher and Glockner (18).

RESULTS AND DISCUSSION

The Exoface Selectants. For the exoface library, we randomly mutated four residues from helix 1 and helix 2 (Ile-17, Leu-20, Leu-23, and Phe-31) that form a hydrophobic core with helix 3 in the intact Z-domain (Fig. 2*A*). After four rounds of binding selection to IgG, a clear consensus was seen (Table 1). The wild-type residues, Leu-20 and Phe-31, were replaced by the charged residues Asp and Lys, respectively (Fig. 2*A*). At the other two positions the wild-type residues, Ile-17 and Leu-23, were predominantly retained, possibly because they stabilize the hydrophobic intraface between helix 1 and helix 2 or the type 1 β-turn that connects them. The consensus exoface 1 selectant (L20D/F31K) had an EC_{50} by phage ELISA of 3.4 μM for binding to IgG (Table 2).The truncated Z-domain peptide (residues 1–38) did not show any detectable binding by phage ELISA, although a K_d in the millimolar range has been reported for an analogous peptide (7).

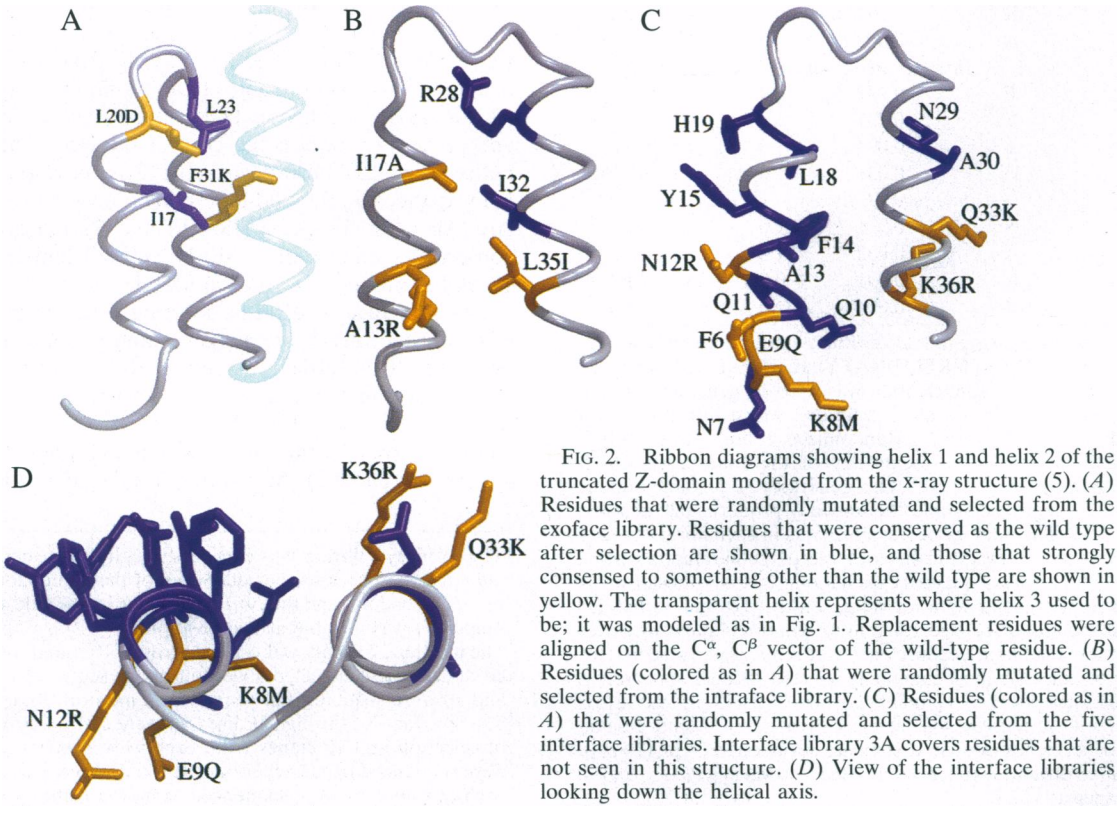

FIG. 2. Ribbon diagrams showing helix 1 and helix 2 of the truncated Z-domain modeled from the x-ray structure (5). (*A*) Residues that were randomly mutated and selected from the exoface library. Residues that were conserved as the wild type after selection are shown in blue, and those that strongly consensed to something other than the wild type are shown in yellow. The transparent helix represents where helix 3 used to be; it was modeled as in Fig. 1. Replacement residues were aligned on the C^α, C^β vector of the wild-type residue. (*B*) Residues (colored as in *A*) that were randomly mutated and selected from the intraface library. (*C*) Residues (colored as in *A*) that were randomly mutated and selected from the five interface libraries. Interface library 3A covers residues that are not seen in this structure. (*D*) View of the interface libraries looking down the helical axis.

Table 1. Consensus residues from each truncated Z-domain library

Wild-type residue	Selected residues	P_e	P_f	$(P_f-P_e)/\sigma$
	*Exoface 1 library**			
I17	I	0.031	0.47	10.5
	A	0.062	0.53	8.1
L20	D	0.031	0.67	15.6
	N	0.031	0.17	3.4
L23	L	0.094	0.94	12.3
F31	K	0.031	0.47	10.5
	F	0.031	0.18	3.5
	Intraface 2 library†			
A13	R	0.094	0.85	11.6
I17	A	0.062	1.0	17.4
R28	R	0.094	1.0	13.9
I32	I	0.031	1.0	24.8
L35	I	0.031	0.90	22.3
	Interface 3A library‡			
D3	A	0.062	0.40	4.4
	R	0.094	0.40	3.3
N4	N	0.031	0.50	8.7
	Q	0.031	0.30	5.0
K5	G	0.062	0.60	7.1
	S	0.094	0.30	2.2
F6	F	0.031	1.0	17.9
	Interface 3B library			
F6	F	0.031	0.60	10.5
	G	0.062	0.40	4.4
N7	N	0.031	0.40	6.8
	W	0.031	0.40	6.8
K8	M	0.031	0.90	16.1
E9	Q	0.031	0.40	6.8
	K	0.031	0.20	3.1
	Interface 3C library			
Q10	Q	0.031	1.0	17.9
Q11	Q	0.031	1.0	17.9
N12	R	0.094	0.70	6.6
	E	0.031	0.20	3.1
R13	R	0.094	0.60	5.5
	A	0.062	0.30	3.1
	Interface 3D library			
F14	F	0.031	1.0	17.9
Y15	Y	0.031	1.0	17.9
L18	L	0.094	1.0	9.8
H19	H	0.031	1.0	17.9
	Interface 3E library			
N29	N	0.031	1.0	17.9
A30	A	0.062	1.0	12.3
Q33	K	0.031	0.80	14.2
K36	R	0.094	1.0	9.8

The sequence of the original 38 residue peptide derived from the Z-domain was AVDNKFNKEQQNAFYEILHLPNLNEEQRNAFIQSLKDD. A single oligonucleotide was used to generate random mutations, except for the intraface 2 library, which introduced two oligonucleotides simultaneously. Randomized codons were synthesized as NNS, where N represents any of the four bases and S represents an equal mix of G/C. This generates 32 possible codons encoding all 20 amino acids and theoretically produces 32^n possible DNA sequences. The number of transformants in each library greatly exceeded the theoretical value in all cases, except the intraface 2 library, where 3.4×10^7 possible sequences exist but only 2×10^6 transformants were obtained. Phagemid libraries were constructed and sorted for binding to immobilized IgG according to *Materials and Methods*. After various rounds of binding selection, clones were sequenced and scored for the number of times the most commonly selected residues appeared at each of the mutated positions. P_e, number of possible NNS codons/32 (for example, Ile is 1/32 and Arg is 3/32, etc.); P_f, number of times residue found/number of clones sequenced; standard deviations $\sigma_n = [P_e(1-P_e)/n]^{1/2}$; n, number of clones sequenced; residues for which $[(P_f-P_e)/\sigma_n] <$ 2.0 are not shown.

Table 2. Phage ELISA and binding kinetics for representative selectants and consensus peptides.

Protein	k_{on}, $\times 10^5 M^{-1}\cdot s^{-1}$	k_{off}, s^{-1}	K_d, nM	EC_{50}, nM
Three helix Z-domain	2.09	0.0021	10	20
Two helix Z-domain	ND	ND	$>1 \times 10^4$	$>1 \times 10^4$
Exoface 1 variant				
A = L20D/F31K	ND	ND	ND	3400
Exoface 1 plus intraface 2 variants				
B = A + I17A/L35A	ND	ND	ND	930
C = A + A13R/I17A/L35I	1.78	0.133	750	420
Exoface 1 plus intraface 2 plus interface 3 variants				
D = C + D3R/K5G	2.06	0.091	440	230
E = C + D3A/N4Q/K5S	1.61	0.091	570	140
F = C + K8M/E9Q	1.48	0.135	910	300
G = C + F6G/N7W/K8M/E9R	2.97	0.099	333	150
H = C + N12R	3.08	0.094	310	180
I = C + N12R/R13A	1.97	0.125	630	260
J = C + Q33K/K36R	2.00	0.073	370	140
Exoface 1 plus intraface 2 plus combined interface 3 variants				
K = D + F + H + J	5.04	0.030	60	180
L = E + F + H + J	4.87	0.030	62	60
M = F6-D38 of L	4.60	0.020	43	ND

Kinetic measurements were determined on a BIAcore where a monoclonal IgG_1 was immobilized on the biosensor chip. The k_{on} values were determined by measuring k_s at five different concentrations, 4, 3, 2, 1, and 0.5 μM and then plotting the K_s values as a function of concentration. Standard error values were <2.5%. The k_{off} values were measured in duplicate with saturating injections at a concentration of 25 μM. Reported values are averaged; standard errors were <3.5%. The K_d values are calculated from k_{off}/k_{on}. Variant M is a synthetic peptide prepared by standard solid phase synthesis using *N*-fluorenyl-methoxycarbonyl protocols. The sequence is FNMQQQRRFYEALHDPNLNEEQRNAKIKSIRDD.

The Intraface Selectants. Starting with the exoface 1 peptide, we generated the interface library by randomly mutating the hydrophobic core between helix 1 and helix 2 (Ala-13, Ile-17, Arg-28, Ile-32, and Leu-35; Fig. 2*B*). Three of the five residues converged (Table 1) to a non-wild-type solution (A13R, I17A, and L35I). These three residues form a cluster and apparently repack the core at the open end of the two helices (Fig. 2*B*). Positions 13 and 17 are next to each other on helix 1; the Ala/Ile wild-type combination is replaced by an Arg/Ala pair. Phage ELISA (Table 2) indicated that the consensus sequence of A13R/I17A/L35I had an EC_{50} about 10-fold improved over the exoface 1 variant.

The Interface Selectants. Starting with the improved exoface/intraface selectant, we generated five interface libraries by randomly mutating nineteen residues, in groups of four, at or near the interface between the Z-domain and the F_c portion of IgG (Fig. 2*C*). For the interface 3A library, a weak consensus was found where Asn-4 and Phe-6 were largely conserved (Table 1). As position 6 is the first ordered contact

*The exoface 1 library was carried through four rounds of selection and 18 clones were sequenced. Seven of the L23 codons found were non-NNS codons, and thus were derived from the wild-type template; one clone was illegible at two positions.

†The intraface 2 library was carried through 10 rounds of selection and 20 clones were sequenced. Five clones were sequenced at round three and 10 were sequenced at round six to monitor library diversity.

‡The interface 3A through 3E libraries were carried through 10 rounds of selection and 10 clones from each were sequenced. Five clones were sequenced from each library at round three, and 10 clones from each at round six were sequenced to monitor library diversity.

residue in the crystal structure (5), this region is not expected to be important for binding.

The interface 3B library generated two different consensus sequences (Table 1); one conserved Phe-6 and Asn-7 while the other mutated these to Gly-6 and Trp-7. The aliphatic portion of Lys-8 in the wild type sits at the helical intraface and does not make direct contact with the IgG; this position showed a strong consensus for Met. Concomitant with the K8M change, the negatively charged Glu-9 was neutralized to Gln or inverted to Lys (Fig. 2*C*).

From the interface 3C library the contact residues, Gln-10 and Gln-11, were completely conserved. Asn-12 was frequently converted to a charged residue (Arg or Glu), while Arg-13 was mostly conserved. The four residues in the interface 3D library were completely conserved, suggesting that these residues cannot be improved upon with natural amino acids. In the interface 3E, two new consensus residues resulted where Gln33 was replaced by Lys, and Lys-36 was replaced by Arg (Fig. 2*D*). Phage ELISA for the consensus selectants from each of these libraries (Table 2) showed improvements in affinity ranging from 2- to 3-fold over the starting exoface/intraface variant.

Improvements in Binding Kinetics and Affinities for the Optimized Peptides. The binding kinetics and affinities for each of the purified consensus peptides were determined to a monoclonal IgG_1 by surface plasmon resonance (Table 2). The starting 38-residue peptide did not show any detectable binding at concentrations up to 25 μM. We estimate that the binding affinity of the combined exoface/intraface selectant (Table 2, variant C) is about 1000-fold improved from the starting 38-residue peptide. Variant C had a k_{on} that was equivalent to the full-length Z-domain but a k_{off} that was $\approx$100-fold greater. This suggests that little structural reorganization is necessary for the analog to bind, but that the binding determinants are not fully optimized relative to the wild-type Z-domain.

The peptides derived from the interface 3 libraries showed slight improvements in k_{on} and/or k_{off} (Table 2, variants D–J). Overall, each showed 2- to 3-fold improvements in affinity over variant C based on comparisons of relative K_d values. To further improve affinity, we combined the consensus variants from the interface libraries (Table 2, variants K and L). These peptides showed 2-fold improvements in k_{on} and a 5-fold improvements in k_{off} relative to most of the selectants in any of the interface 3 libraries. The affinities for these mutants are only 6-fold weaker than the full-length Z-domain and represent an improvement of $>10^4$-fold over the starting 38-residue peptide. These final derivatives associate about 2.5-times faster than the full-length Z-domain and dissociate only about 14-fold faster, suggesting that the optimization of the binding determinants on the analog is approaching that of the full-length Z-domain. A synthetic peptide derived from variant L but with the N-terminal five residues deleted (Phe-6–Asp-38, variant M) actually has a slower k_{off} than variant L and thus a K_d value only 4-fold higher than the Z-domain. This peptide has now been reduced to only 33 residues, sequence FNMQQQRRFYEALHDPNLNEEQRNAKIKSIRDD from the original 59 residue Z-domain.

Evolving Binding Affinity in the Two-Helix Derivative Increases the α-Helical Structure. The secondary structural characteristics of some of these peptides after various stages of affinity optimization were evaluated by CD spectroscopy (Fig. 3). The starting 38-residue peptide showed only 11% helical content. However, the helical content progressively increased in going from this to the exoface/intraface optimized variant (50%) and then to the final combined interface mutant (56%). This compares with a maximum helical content of 63% estimated from the number of residues in a helical conformation as determined from the x-ray coordinates (5) of the two-helix segment present in the intact B-domain.

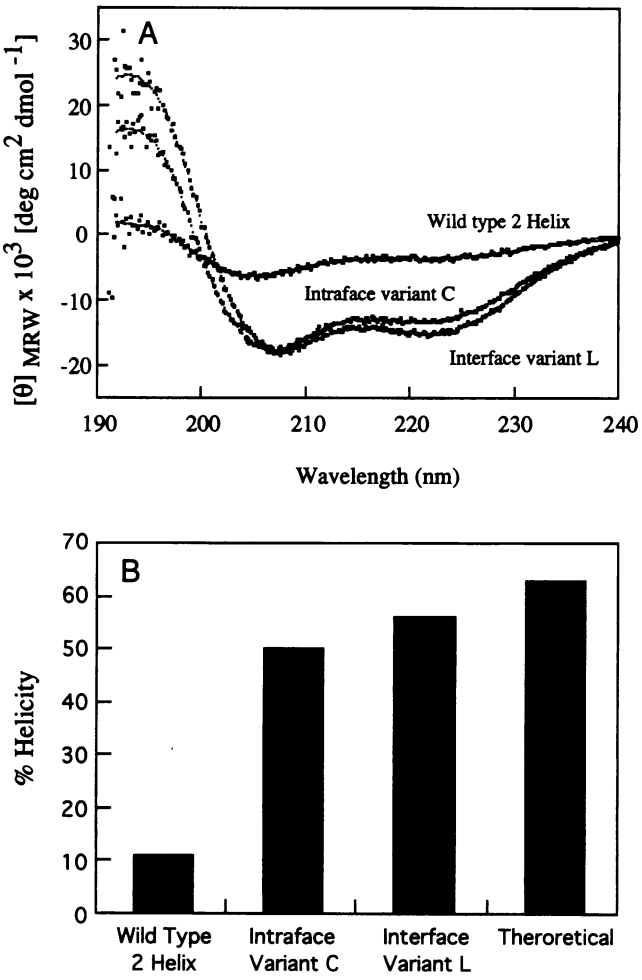

FIG. 3. CD spectra of the starting 38-residue peptide, and the intraface and interface optimized peptides (*A*). Data were collected and curves fit as described. The extent of helicity was calculated for these peptides directly from the CD spectra (*B*). These values can be compared to the theoretical maximum value as determined by inspection of the structure of the first two-helices in the intact B-domain.

Additional evidence suggests that the evolved two-helix bundle is highly structured. First, the k_{on} values are comparable to or greater than the full-length Z-domain, suggesting little reorganization is necessary. Many of the residues that are selected in either the exoface, intraface, or interface libraries are buried in the two-helix bundle model (Fig. 2). These likely are selected because they stabilize the core of the two-helix structure. Many of the residues that were absolutely conserved in the interface libraries are seen highly buried in the complex with the IgG, suggesting that determinants from the two-helix motif are the same ones used in the full-length Z-domain. This has been recently confirmed by alanine-scanning mutagenesis of the two-helix variant L which shows that these conserved residues are critical for binding (unpublished data). Lastly, binding from a discontinuous epitope usually depends on precise display of determinants and therefore requires a highly ordered structure (19. 20). Preliminary results from the structural characterization of a two helix variant by NMR (M. Starovasnik, A.C.B., and J.A.W., unpublished data) confirm that this peptide adopts essentially the same conformation as helix 1 and helix 2 in the x-ray structure (5).

CONCLUSIONS

We have shown it is possible to substantially reduce the size of a protein domain while preserving its binding function even

when the binding epitope is discontinuous—typical of most protein–protein interfaces. Reducing a discontinuous epitope is a much more difficult task than for reduction of a continuous epitope such as the RGD motif that bind integrins. To retain a continuous epitope, only the local structure around a small sequence motif needs to be preserved. This strategy for reducing the size of protein domains displaying discontinuous epitopes has also been recently applied to a polypeptide hormone, atrial natriuretic peptide (ANP), which consists of loops connected by a disulfide bond (21). It was possible to reduce ANP from 28 residues to 14 while maintaining high affinity and biopotency.

The minimization of the Z-domain could have important applications since protein A is useful for the purification of antibodies and F_c-fusion proteins (22). The mini-Z-domain is more synthetically accessible and therefore may be further improved with non-natural substitutions. More generally these results suggest that protein domains are not indivisible elements of stable protein structure—smaller functional versions can be produced.

We thank Dr. Michael Mulkerrin for help with the CD analysis, David Wood for the molecular graphics, Allan Padua for amino acid analysis, and the oligonucleotide synthesis group.

1. Doolittle, R. F. (1992) *Protein Sci.* **1,** 191–200.
2. Bork, P. (1992) *Curr. Opin. Struct. Biol.* **2,** 413–421.
3. Nilsson, B., Moks, T., Jansson, B., Abrahamsen, L., Elmblad, A., Holmgren, E., Henrichson, C., Jones, T. A. & Uhlén, M. (1987) *Protein Eng.* **1,** 107–113.
4. Cedergren, L., Andersson, R., Jansson, B., Uhlén, M. & Nilsson, B. (1993) *Protein Eng.* **6,** 441–448.
5. Deisenhofer, J. (1981) *Biochemistry* **20,** 2361–2370.
6. Gouda, H., Torigoe, H., Saito, A., Sato, M., Arata, Y. & Shimada, I. (1992) *Biochemistry* **31,** 9665–9672.
7. Huston, J. S., Cohen, C., Maratea, D., Fields, F., Tai, M. S., Cabral-Denison, N., Juffras, R., Rueger, D. C., Ridge, R. J., Oppermann, H., Keck, P. & Baird, L. G. (1992) *Biophys. J.* **62,** 87–91.
8. Smith, G. P. (1991) *Curr. Opin. Biotechnol.* **2,** 668–673.
9. Clackson, T. & Wells, J. A. (1994) *Trends Biotechnol.* **12,** 173–183.
10. Nord, K., Nilsson, J., Nilsson, B., Uhlén, M. & Nygren, P. (1995) *Protein Eng.* **8,** 609–614.
11. Djojonegoro, B. M., Benedik, M. J. & Willson, R. C. (1994) *Bio/Technology* **12,** 169–172.
12. Lowman, H. B. & Wells, J. A. (1991) *Methods Companion Methods Enzymol.* **3,** 205- 216.
13. Kunkel, T. A., Bebnek, K. & McClary, J. (1991) *Methods Enzymol.* **204,** 125–139.
14. Cunningham, B. C., Lowe, D. L., Li, B., Bennett, B. D. & Wells, J. A. (1994) *EMBO J.* **13,** 2508–2515.
15. Chang, C. N., Rey, M., Bochner, B., Heyneker, H. & Gray, G. (1987) *Gene* **55,** 189–196.
16. Johnsson, B., Löfås, S. & Lindquist, G. (1991) *Anal. Biochem.* **198,** 268–277.
17. Karlsson, R., Michaelson, A. & Mattson, A. (1991) *J. Immunol. Methods.* **145,** 229–240.
18. Provencher, S. W. & Glockner, J. (1981) *Biochemistry* **20,** 33–37.
19. Epand, R. M. & Scheraga, H. A. (1968) *Biochemistry* **7,** 2864–2872.
20. Tsou, C. L. (1993) *Science* **262,** 380–381.
21. Li, B., Tom, J. Y. K., Oare, D., Yen, R., Fairbrother, W. J., Wells, J. A. & Cunningham, B. C. (1995) *Science* **270,** 1657–1660.
22. Uhlén, M., Forsberg, G., Moks, T., Hartmanis, M. & Nilsson, B. (1992) *Curr. Opin. Biotechnol.* **3,** 363–369.